Biochimica et Biophysica Acta, 1103 (1992) 239–249

BBAMEM 75493

Transport and metabolism of palmitate in the rat liver. Net flux and unidirectional fluxes across the cell membrane

O. Ferraresi-Filho [1], M. Ferraresi [1], J. Constantin [1], E.L. Ishii-Iwamoto [1], J. Schwab [2] and A. Bracht [1]

[1] *Laboratory of Liver Metabolism, University of Maringá, Maringá (Brazil) and* [2] *McGill University Medical Clinic, Montreal General Hospital, Montreal (Canada)*

(Received 29 May 1991)
(Revised manuscript received 17 September 1991)

Key words: Palmitate; Membrane transport; Multiple-indicator dilution technique; Fatty acid metabolism; Unidirectional flux; (Rat liver)

The unidirectional fluxes of palmitate across the liver cell membrane and metabolic uptake rates were measured employing the multiple-indicator dilution technique. The following results were obtained: (1) Influx and net uptake rates do not vary proportionally to each other when albumin and palmitate concentrations are varied. (2) Efflux is significant for albumin concentrations in the range between 1.5 and 500 μM. (3) At 150 μM albumin net uptake rates are proportional to the total (bound plus free) extracellular palmitate concentration in the range from 10 to 600 μM; the dependence of influx rates on the palmitate concentration is rather concave up. (4) When albumin and palmitate are both varied at an equimolar ratio, pseudo-saturation appears in the net uptake rates; the influx rates also show pseudo-saturation, but with a declining tendency at the higher concentrations. (5) The intracellular palmitate concentration is strongly influenced by albumin. At very low concentrations of the protein (1.5 μM) the intracellular concentration is practically equal to the extracellular one; at physiological albumin concentrations, however, the intracellular palmitate concentration is less than 2% of the extracellular one. (6) Saturation of net uptake with respect to the intracellular palmitate concentration was not observed with concentrations up to 46 μM.

Introduction

The uptake of fatty acids and of other albumin-bound substances by the liver cells has been the subject of intense investigation in the last years. Two main interrelated questions have been under discussion: the limiting factors for net uptake and the mechanism of permeation. The early conjecture of the involvement of a specific albumin receptor at the surface of the liver cells [1–4] was later abandoned, because its existence could not be confirmed [5]. More accurate modeling of the overall uptake process revealed that the kinetics of uptake could also be explained, partly at least, by extracellular events far from the cell surface. In the case of a whole organ, where the ratio of extra- to intracellular spaces is low, replacement of free substrate by dissociation of the albumin-fatty acid complex may become rate-limiting [4]. Moreover, it has also been demonstrated that permeation of the cell membrane occurs by means of a carrier which binds and transports the free form of long-chain fatty acids [6,7], a fact which also influences the overall uptake kinetics.

In most studies on fatty acids uptake in the perfused liver, influx has not been measured directly. Net uptake rates have been measured instead and assumed to be (a) equal to or at least (b) proportional to influx rates. In the first case, it is implied that influx is rate-limiting for uptake [1,8]; in the second case, it is implicitly or explicitly assumed that the ratios of influx to efflux rates remain constant [2,9]. The assumption that influx is strictly rate-limiting i.e. metabolism is certainly incorrect. This was shown by Goresky et al. [10] in the liver of anesthetized dogs, where the rate constants for transport and metabolism of tracer [1-^{14}C]palmitate were measured by means of the multiple-indicator dilution technique. From these studies it could be concluded that, at least at physiological albumin concentrations, uptake is not solely determined by the influx rate, but that intracellular factors are equally important. Proportionality between influx

Correspondence: A. Bracht, Laboratory of Liver Metabolism, University of Maringá, P.O. Box 331, 87020 Maringá, Brazil.

and efflux is also unlikely under steady-state conditions, especially in the case of carrier mediated transport [10], where the kinetic constants for influx and efflux are functions of the concentrations of the solute on both sides of the membrane [11,12]. Experimentally, however, this is still an open question, because the steady-state unidirectional fluxes have not yet been measured in the perfused liver. The measurement of these fluxes is precisely the scope of the present work. Studies of this kind are best performed in the isolated liver, where albumin and palmitate concentrations can be freely varied. The experimental procedure employed was the multiple-indicator dilution technique described by Goresky and co-workers [10,13] for the liver of the anesthetized dog and adapted to the hemoglobin-free perfused rat liver by the group of Scholz [14]. With this technique the transport of several compounds has been successfully investigated in the liver [10,14–18].

A minor part of the results described in this work has already been published as a short communication [19].

Materials and Methods

Hemoglobin-free liver perfusion

Male albino rats (Wistar strain; 220–300 g) received a standard laboratory diet (Purina) and water ad libitum prior to the surgical removal of the liver under pentobarbital anesthesia (50 mg/kg body weight). The perfusion technique described by Scholz et al. [20] was used. The perfusion fluid was Krebs/Henseleit-bicarbonate buffer (pH 7.4) saturated with an oxygen/carbon dioxide mixture (95:5, v/v). It contained fatty acid-free serum albumin (1.5 to 500 μM) and palmitate (10 to 600 μM), according to the experimental protocol. The fluid was pumped through a temperature-regulated (37 °C) membrane oxygenator before entering the liver via a cannula inserted into the portal vein. The effluent perfusate flowed past an oxygen electrode before being discarded, or, in multiple-indicator dilution experiments, collected by a fraction collector. The flow rate was adjusted to the metabolic activity of the liver as judged from the venous oxygen concentration. It varied between 4 and 5 ml/min per g, but was constant in each individual experiment. Viability of the livers was judged from rates of oxygen uptake.

Multiple-indicator dilution experiments

Multiple-indicator dilution experiments were performed by injecting 350 μl of a mixture containing [1-^{14}C]palmitate (2 μCi), ^{131}I-albumin (0.2 μCi) and [^{3}H]water (20 μCi). In addition to labeled substances, the injected solution also contained fatty acid free albumin and palmitate at concentrations equal to those in the influent perfusate. The effluent perfusate was collected in 0.5- to 2.0-s fractions over a period of 90 s following injection by means of a especially designed fraction collector [14]. Injections were performed between 6 and 12 min after the onset of the perfusion with Krebs/Henseleit-bicarbonate buffer containing unlabeled albumin and palmitate, leaving enough time for the attainment of steady-state conditions, as judged from oxygen uptake measurements.

Analytical

The fractions of the effluent perfusate were divided into two aliquots. One aliquot was used for the determination of ^{131}I albumin and [^{3}H]water by means of liquid scintillation spectrometry. [1-^{14}C]Palmitate was extracted from the second aliquot according to Dole and Meinertz [21]. From each fraction, an aliquot of 200 μl was extracted with 1.0 ml of a mixture containing 0.5 M HCl, *n*-heptane and isopropanol (0.1:1:4, v/v). The mixture was vigorously shaken for 30 s. After 5 min, 0.4 ml water and 0.6 ml *n*-heptane were added. After shaking the resulting mixture, 0.7 ml of the upper phase were pipetted into scintillation vials for radioactivity measurement. The scintillation solution contained toluol/Triton X-100 (10:5.5, v/v) and 5.0 g/liter of 1,5-diphenyloxazole(PPO) plus 0.2 g/liter 2,2'-*p*-phenylene-bis[5-phenyloxazole] (POPOP). The radioactivity in the perfusate was expressed as the fraction of the total radioactivity of each labeled substance injected that was recovered per second. The amount of injected [1-^{14}C]palmitate was determined from the injected and recovered ratios of [1-^{14}C]palmitate to ^{131}I-albumin. The injected ^{131}I-albumin radioactivity was assumed to be equal to the recovered one [13].

Material

The liver perfusion apparatus and the fraction collector for multiple-indicator dilution experiments were built in he workshops of the University of Maringá according to a model first developed in Munich in the Institut für Physiologische Chemie [14]. Fatty acid-free bovine serum albumin was purchased from Sigma Chemical Company (St. Louis, MO). The reagent grade chemicals were from Merck (Darmstadt, F.R.G.), Carlo Erba (São Paulo, Brazil) and Reagen (Rio de Janeiro, Brazil).

The following radiochemicals were purchased from E.I. du Pont de Nemours & Co. (Boston, MA): [^{3}H]water (NET-001C, 25 mCi/g), [1-^{14}C]palmitic acid (NEC-075, 2-10 mCi/mmol; and NEC-075H, 40–60 mCi/mmol). ^{131}I-Albumin was purchased from the Comissão Nacional de Energia Nuclear (São Paulo, Brazil).

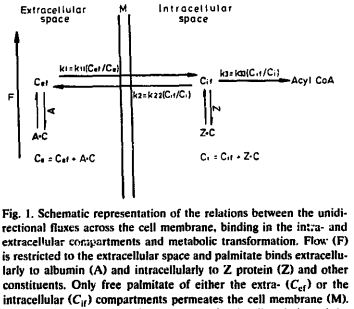

Fig. 1. Schematic representation of the relations between the unidirectional fluxes across the cell membrane, binding in the intra- and extracellular compartments and metabolic transformation. Flow (F) is restricted to the extracellular space and palmitate binds extracellularly to albumin (A) and intracellularly to Z protein (Z) and other constituents. Only free palmitate of either the extra- (C_{ef}) or the intracellular (C_{if}) compartments permeates the cell membrane (M). Free palmitate is constantly regenerated by the dissociation of the albumin-palmitate complex (A·C) or the Z protein-palmitate complex (Z·C). The total (bound plus free) extra- and intracellular palmitate concentrations are represented by C_e and C_i, respectively. The measurable rate constants for influx (k_1), efflux (k_2) and metabolic transformation (k_3) are composite rate constants, products of the rate constant for the transport or metabolic transformation of free palmitate (k_{11}, k_{22} and k_{33}) with the fraction of free palmitate (i.e., C_{ef}/C_e or C_{if}/C_i) [10]. Furthermore, the rate constants for transport or metabolic transformation of free palmitate are, respectively, functions of the kinetic constants of the transport system [12,15–18] and of the enzymic system [22,23].

Calculations

The outflow profiles of labeled [1-^{14}C]palmitate obtained from the indicator-dilution experiments were analyzed employing the space-distributed variable transit-time model proposed by Goresky and co-workers [10,13,17]. According to this model, the outflow profiles of labeled [1-^{14}C]palmitate, $Q(t)$, can be described by a function which contains the outflow profile of a reference substance ($Q_{ref}[t]$) representing the heterogeneity of the sinusoidal transit times (τ), the transit time in the large vessels (t_0), the ratio of intracellular to extracellular volumes of the liver (θ'), and the parameters for the transport across the plasma membrane (k_1, influx; k_2, efflux) and for metabolic sequestration (k_3) of labeled palmitate:

$$Q(t) = Q_{ref}(t)\exp[-k_1\theta'(t-t_0)] + \exp[-(k_2+k_3)(t-t_0)] \cdot \int_0^{t-t_0} \exp[(k_2+k_3-k_1\theta')\tau]\cdot Q_{ref}(\tau+t_0) \cdot \sum_{n=1}^{\infty} \frac{(k_1k_2\theta'\tau)^n(t-t_0-\tau)^{n-1}}{(n!)(n-1)!}\,d\tau \quad (1)$$

Fig. 1 illustrates the relationships between the unidirectional fluxes, binding in the intra- and extracellular spaces and metabolic transformation. Flow (F) is restricted to the extracellular space and palmitate binds extracellularly to albumin (A) and intracellularly to Z protein (Z) and other constituents [10]. Only free palmitate of either the extra- (C_{ef}) or the intracellular (C_{if}) compartments permeates the cell membrane (M). Free palmitate, however, is constantly regenerated by the dissociation of the albumin-palmitate complex (A·C) or the Z protein-palmitate complex (Z·C). The total (bound plus free) extra- and intracellular palmitate concentrations are represented by C_e and C_i, respectively. The measurable rate constants for influx (k_1), efflux (k_2) and metabolic transformation (k_3) are, consequently, composite rate constants, products of the rate constant for the transport or metabolic transformation of free palmitate (k_{11}, k_{22} and k_{33}) with the fraction of free palmitate (i.e., C_{ef}/C_e or C_{if}/C_i) [10]. Furthermore, the rate constants for transport of free palmitate (k_{11} and k_{22}) are functions of the kinetic constants of the transport system [12,15–18]. And, finally, the rate constant for metabolic transformation of free palmitate (k_{33}) is a function of the kinetic constants of acyl-coenzyme A synthetase as well as of the metabolic state of the liver in terms of energy metabolism and the availability of free coenzyme A [22,23]. The dimensions of k_1 are ml perfusate per s per ml intracellular water space^{-1}; and that of k_2 and k_3 are ml intracellular phase per s per ml intracellular space [18].

Steady-state rates can be calculated by multiplying the rate constants by the corresponding concentrations. The rates that can be calculated are influx ($F_1 = k_1C_e$), efflux ($F_2 = k_2C_i$) and net flux (metabolic transformation, $F_3 = k_3C_i$). C_e can be determined as the logarithmic mean of the portal and hepatic venous extracellular concentrations, calculated according to Goresky et al. [24] and C_i is the steady-state intracellular concentration. The latter can be calculated from C_e and the rate constants by the following expression [18]:

$$C_i = \frac{k_1}{k_2+k_3}C_e \quad (2)$$

The rate of metabolic transformation can also be calculated from the portal-venous concentration difference and the mean transit times ($\bar{t}$) of [^{3}H]water and [^{131}I-albumin [25]:

$$F_3^* = \frac{C_p - C_v}{\bar{t}_{water} - \bar{t}_{alb}} \quad (3)$$

C_p and C_v are the portal and venous palmitate concentrations, respectively. All rates calculated from the rate constants or from Eqn. 3 are referred to the intra-

cellular water space. It should be noted that Eqn. 3 provides a mean of calculating the metabolic flux which is independent of Goresky's model.

The rate constants for influx, efflux and metabolic sequestration were obtained by fitting Eqn. 1 to the fractional outflow profiles of labeled palmitate using an iterative non-linear least-squares procedure [26,27]. Iteration was continued until the sum of squares of the differences between the experimental and calculated [1-^{14}C]palmitate outflow profiles was a minimum. For calculating Eqn. 1, an extravascular reference curve is needed as well as values for t_0 and θ'. The reference curve used in this work was the outflow profile of ^{131}I-albumin. Interpolation between the experimental points of the reference curve was performed by means of a spline-function [26]. Values for t_0 and θ' were derived from the superposition of the fractional outflow profiles of [^{3}H]water and ^{131}I-albumin, following a linear transformation proposed by Goresky [13]. The superposition of the [^{3}H]water and ^{131}I-albumin curves was optimized by a non-linear least-squares procedure [13,26]. The integral of Eqn. 1 was calculated by means of Romberg's algorithm [26]. The time integrals and the mean transit times of the fractional outflow profiles were determined by the trapezoid rule with monoexponential extrapolation to infinite time [26]. The equilibrium free palmitate concentrations were calculated according to the algorithm of Abumrad et al. [28], using the equilibrium constants measured by Spector et al. [29].

Results

Typical outflow dilution curves of [1-^{14}C]palmitate and indicators

Fig. 2 illustrates the outflow profiles from four typical palmitate experiments performed with various albumin and palmitate concentrations. All curves were normalized by dividing the amount of radioactivity recovered in each fraction by the injected radioactivity and by the collection time interval. When normalized in this way, the area under each of the indicator curves, ^{131}I-albumin and [^{3}H]water, becomes equal to unity. Characteristically, the [1-^{14}C]palmitate curve is always contained within the envelope of the ^{131}I-albumin curve. Figs. 2A and 2D illustrate the two extremes found by changing the palmitate and albumin concentrations. In Fig. 2A (500 μM albumin; 500 μM palmitate), extraction is low (19%) and the peak of the labeled palmitate curve coincides with that of the labeled albumin curve. In Fig. 2D (1.5 μM albumin; 10 μM palmitate), the extraction is high (80%) and the peak of the labeled palmitate curve precedes that of labeled albumin by two seconds. This shift in the peak of the [1-^{14}C]palmitate curve relative to the ^{131}I-albumin curve is a general trend when the albumin concentration is lowered (see Fig. 2C). The experiments shown in Figs. 2A–2D were performed with various palmitate concentrations, but the changes in the outflow profiles are mainly due to the different albumin concentrations. The curves in Fig. 2B, for example, were obtained with 150 μM albumin and 300 μM palmitate, but they are representative for all portal palmitate concentrations in the range from 10 to 600 μM, with only minor variations.

Since the experiments were all performed under steady-state conditions, the extraction of the injected tracer is proportional to the portal-venous concentration difference. From the latter and the mean transit times of the indicators, the rate of net uptake can be calculated according to Eqn. 3. The calculation of the unidirectional fluxes and the intracellular palmitate pools, however, cannot be made without more extensive mathematical modeling.

Analysis and resolution of the [1-^{14}C]palmitate outflow profiles

The fit of Eqn. 1 to the outflow profiles of [1-^{14}C]palmitate is illustrated in Table 1 and Fig. 2. A short description of the meaning of the parameters in Eqn. 1 can be found in Materials and Methods and in the legend to Fig. 1. Table 1 allows a statistical evaluation of the reproducibility of the values of k_1, k_2 and k_3 at various combinations of palmitate and albumin concentrations. The rate constant for influx, k_1, presents the lowest standard errors, but those of k_3 are also relatively small. From the three parameters, k_2 is the rate constant which can be determined with the least precision, but the standard errors generally remain within tolerable limits. The rate constants vary considerably, especially k_2, which ranges from 0.038 to 1.30 ml intracellular phase per s per ml intracellular space, depending on the experimental conditions. A situation in which $k_3 \gg k_2$, meaning strict limitation of net uptake by transport, was not observed. The maximal difference between both rate constants ($k_3/k_2 = 5.7$) was found at 10 μM palmitate and 1.5 μM albumin.

Fig. 3A illustrates how Eqn. 1, with optimized values for t_0, θ', and the rate constants, describes a representative experimental outflow profile of [1-^{14}C]palmitate. The calculated curve (solid line in Fig. 3A) is in good agreement with the measured outflow profile. Goresky et al. [10] obtained similar good fits in experiments performed in the liver from anesthetized dogs. The model is, thus, a good approximation of the phenomena following a pulse injection of labeled palmitate into the liver. Fig. 3A also shows the resolution of the outflow profile into its components: (a) the throughput component, given by the first term in Eqn. 1, which is the material that had no access to the intracellular space during a single passage through the liver; and,

(b) the exchanged component, given by the second term in Eqn. 1, which corresponds to the material that has entered the liver cells, but has escaped from metabolic transformation. The significance of this fraction can be evaluated more precisely by the type of representation adopted in Fig. 3B, which shows the cumulative outflow, obtained by integration of the curves of Fig. 3A. Recovery of label at the venous outflow is 61% and is attained within 40 s after injection. The exchanged component represents 39% of the recovered material.

Due to the equivalence between continuous infusion and single injection in indicator-dilution experiments [13,25], in the absence of palmitate production by the liver, the cumulative outflow curves shown in Fig. 3B tend asymptotically to values which reflect the steady-state conditions in the effluent perfusate in terms of the bulk palmitate concentration. The proportions of the components shown in Fig. 3B are valid for the specific experimental conditions of the experiment (150 μM albumin; 300 μM palmitate). In view of the pronounced changes in the outflow profiles of labeled

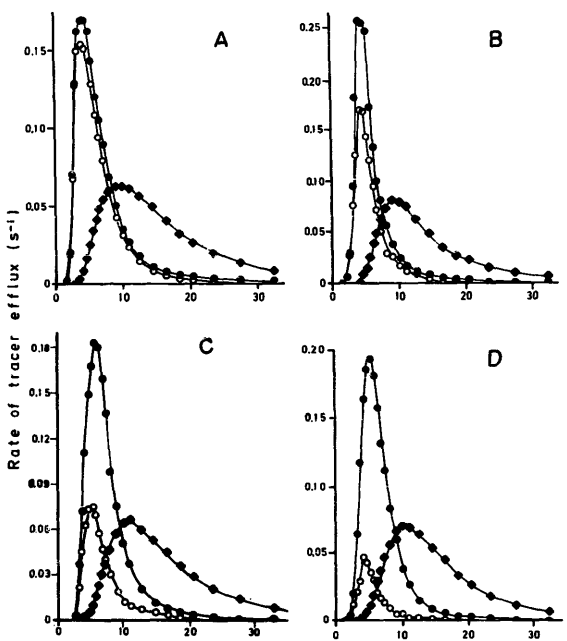

Fig. 2. Outflow profiles of [1-^{14}C]palmitate and indicator substances under various conditions. Livers from fed rats were perfused with Krebs/Henseleit-bicarbonate buffer (pH 7.4) containing albumin and palmitate at the concentrations indicated below. In each experiment, trace amounts of [1-^{14}C]palmitate (○——○), ^{131}I-albumin (●——●) and [^{3}H]water (◆——◆) were simultaneously injected into the perfusate prior to entering the liver. The effluent perfusate was collected in 0.5–2.0-s fractions. The fractions of the injected radioactivity which appeared per second were plotted versus the time following injection. Key: (A) 500 μM albumin; 500 μM palmitate; (B) 150 μM albumin; 300 μM palmitate; (C) 10μM albumin; 10 μM palmitate; (D) 1.5 μM albumin; 10 μM palmitate.

TABLE I

Mean values of rate constants, extraction, exchanged component, throughput component, and C_i/C_e values (equivalent to $k_1/[k_2+k_3]$) for several sets of experiments performed at various palmitate and albumin concentrations

The rate constants were obtained by fitting Eqn. 1 to the outflow profiles of labeled palmitate as described in Materials and Methods. The dimensions of k_1 are ml perfusate per s per ml intracellular water space; and those of k_2 and k_3 are ml intracellular phase per s per ml intracellular space. The values represent the means ±S.E.

Portal palmitate (μM)	Albumin (μM)	k_1	k_2	k_3	C_i/C_e	Single pass extraction (%)	Recovery		Total (%)
							throughput (%)	exchanged (%)	
10 ($n=3$)	1.5	0.282±0.011	0.038±0.006	0.195±0.042	1.29 ±0.18	76.9±3.1	15.8±2.3	7.4±2.4	100.1
10 ($n=3$)	10	0.300±0.057	0.446±0.156	0.507±0.105	0.34 ±0.04	67.4±2.3	16.8±3.9	16.1±3.1	100.3
100 ($n=3$)	15	0.146±0.012	0.240±0.099	0.415±0.072	0.26 ±0.06	50.9±1.2	34.4±2.9	14.4±2.9	99.7
200 ($n=3$)	150	0.122±0.012	1.30 ±0.11	0.652±0.012	0.069±0.007	30.9±3.8	37.5±2.8	31.3±1.1	99.7
350 ($n=3$)	150	0.124±0.023	0.904±0.45	0.653±0.084	0.088±0.017	35.6±1.8	38.4±8.4	25.0±6.6	99
350 ($n=4$)	350	0.040±0.004	0.447±0.09	0.798±0.283	0.048±0.008	20.2±1.5	74.0±5.7	7.2±3.4	101.4

palmitate shown in Fig. 2, which reflect in the rate constants as shown in Table I, one can also expect alterations in the relative proportions of the throughput and exchanged components. To illustrate this, Table I shows, in addition to the computed rate constants, mean values for extraction, for the resolved recovery (throughput and exchanged) and for the C_i/C_e ratio. As expected from the variation of the rate constants, the proportions between extraction, throughput and exchanged components vary considerably. From the experiments shown in Table I, the condition 1.5 μM albumin and 10 μM palmitate is one extreme: high extraction, low throughput and a high C_i/C_e ratio. For the other extreme, 350 μM albumin and 350 μM palmitate, extraction is low, the throughput high and the C_i/C_e ratio very low. The exchanged component is similar for these two extremes, but for the low albumin condition it performs 31.5% of the recovery; and in the high albumin condition it amounts to less than 10% of the recovery. The C_i/C_e is strongly influenced by the albumin concentration, as can be concluded by comparing experiments with identical palmitate concentrations, but different albumin concentrations.

Table I also presents the sum of extraction plus the two components of the recovery, which is in all cases very close to 100%. Extraction is an experimental pa-

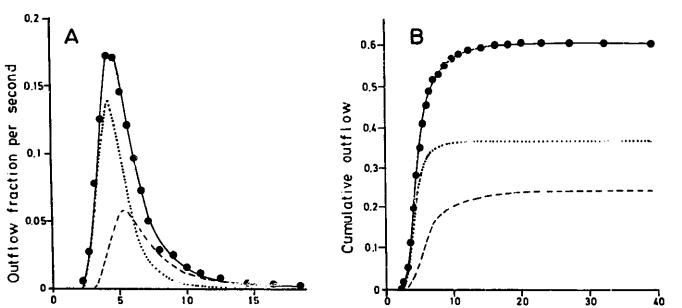

Fig. 3. Experimental and theoretical outflow profiles (A) and cumulative outflow curves (B) of [1-^{14}C]palmitate. The experimental [1-^{14}C]palmitate curve (●———●) is that one shown in Fig. 2B, with 150 μM albumin and 300 μM palmitate in the perfusate. The solid lines (———) represent the theoretical outflow profile (A) or the theoretical cumulative outflow curve (B), calculated according to Eqn. 1 with the following parameters: $\theta' = 2.11$; $t_0 = 2.1$ s; $k_1 = 0.127$ ml perfusate per s per ml intracellular water space; $k_2 = 0.893$ ml intracellular phase per s per ml intracellular space; and, $k_3 = 0.668$ ml intracellular phase per s per ml intracellular space. The dotted lines (·····) represent the resolved throughput component, which is given by the first term of Eqn. 1. The broken lines (- - - - -) represent the exchanged component, given by the second term in Eqn. 1.

rameter, but the throughput and the exchanged components were computed from Eqn. 1, using optimized parameters. The sum of these components with the extraction must approach 100% if Eqn. 1 is a good description of the outflow profiles of [1-^{14}C]palmitate.

Concentration dependences of unidirectional fluxes, net flux and intracellular to extracellular ratio

The net flux can be computed independently from the rate constants (F_3) or from Eqn. 3 (F_3^*). In a series of 43 experiments the mean ratio F_3/F_3^* was equal to 1.11 ± 0.04. One can expect that the difference between F_3 and F_3^* increases when extraction is high, because this also increases the number of sinusoids in which the cells situated at the perivenous zone do not receive any palmitate. This is valid for the sinusoids with high transit times [17]. In fact, if one calculates the mean F_3/F_3^* ratio for those experiments in which extraction was less than 50%, one arrives at a value of 1.05 ± 0.05 ($n = 37$). Agreement between both values is thus within reasonable limits.

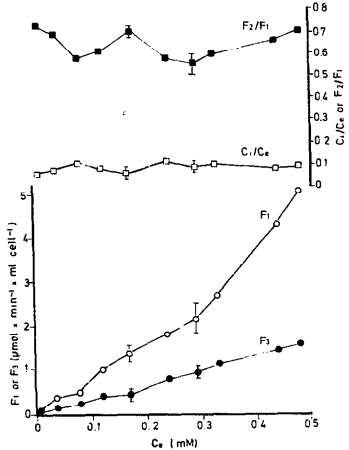

Fig. 4. Dependence of influx (F_1), net uptake (F_3), the ratio of intra- to extracellular concentration (C_i/C_e) and the ratio of efflux to influx (F_2/F_1) on the extracellular palmitate concentration (C_e) at a fixed albumin concentration (0.15 mM). Values for the variables were calculated according from the rate constants as described in Materials and Methods. The rate constants were obtained by fitting Eqn. 1 to the outflow profiles of [1-^{14}C]palmitate, measured in 14 liver perfusion experiments in which the concentration of portal palmitate was varied in the range between 10 and 600 μM and the concentration of albumin was equal to 150 μM.

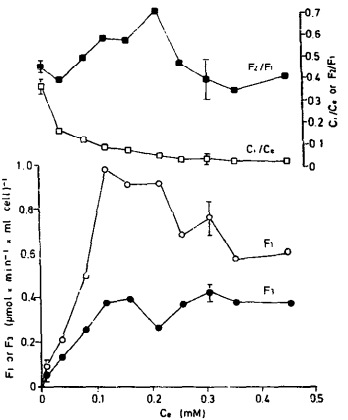

Fig. 5. Dependence of influx (F_1), net uptake (F_3), the ratio of intra- to extracellular concentration (C_i/C_e) and the ratio of efflux to influx (F_2/F_1) on the extracellular palmitate concentration (C_e) with simultaneous variation of the palmitate and albumin concentrations at an equimolar ratio. The values for the variables were calculated from the rate constants as described in Materials and Methods. The rate constants were obtained by fitting Eqn. 1 to the outflow profiles of [1-^{14}C]palmitate, measured in 15 liver perfusion experiments in which the portal concentrations of palmitate and albumin were simultaneously varied in the range between 10 and 500 μM at an equimolar ratio

The kinetics of palmitate influx was analyzed by means of the two most commonly employed experimental protocols: (a) variation of the concentration of the ligand at a fixed albumin concentration, and (b) simultaneous variation of the concentrations of both ligand and albumin at an equimolar ratio [1–4,8]. Fig. 4 shows the results of the experiments with 150 μM albumin and variable palmitate concentrations in the range between 10 and 600 μM portal palmitate. The values of influx rates, net uptake rates, C_i/C_e and F_2/F_1 were plotted versus the mean extracellular palmitate concentration (C_e). The relation between the net uptake rates and C_e is approximately linear, but that between the influx rates and C_e is rather concave up. Fig. 4 also reveals a more or less constant ratio of efflux to influx and a constant proportion between the intra- and extracellular concentrations (top panel). The mean value for F_2/F_1 is 0.635 ± 0.019 ($n = 14$), indicating that at 150 μM albumin, uptake is limited

predominantly by intracellular factors. The intracellular concentration is much lower than the extracellular one, the mean value of the C_i/C_e ratio being equal to 0.084 ± 0.007 ($n = 14$).

The results of the series of experiments in which the concentrations of palmitate and albumin were varied at an equimolar ratio are shown in Fig. 5. The same type of representation as that in Fig. 4 was adopted. F_3 shows a kind of pseudo-saturation, as previously found for oleate by Weisiger et al. [1]. F_1 also shows pseudo-saturation, however, instead of stabilizing at the highest concentrations it decreases again. The concentration dependence of the F_2/F_1 ratio also reveals complexities. It increases initially with C_e, but after a maximum between 200 and 250 μM it decreases again. The C_i/C_e ratio, finally, decreases progressively as the extracellular palmitate-albumin concentrations are raised. From the initial value of 0.34, at the lowest palmitate-albumin concentrations (10 μM), it becomes less than 0.02 at the highest concentrations (500 μM).

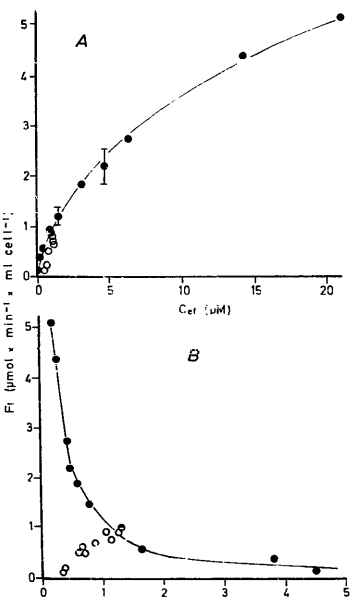

Fig. 6. Rates of influx of palmitate as a function of the equilibrium free palmitate concentration (C_{ef}). The free palmitate concentrations were calculate as described in Materials and Methods. The data points are (a) from the series of experiments with constant albumin (150 μM) and variable palmitate concentrations (10–600 μM in the portal vein; ●——●) and (b) from the series of experiments in which palmitate and albumin were varied at an equimolar ratio (10–550 μM in the portal vein, ○). (A) F_1 versus C_{ef}; (B) the Hofstee plot, i.e., F_1 versus F_1/C_{ef}.

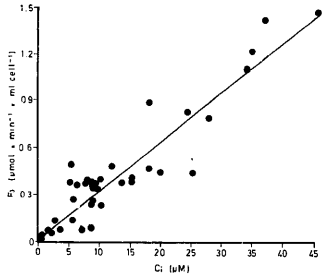

Fig. 7. Dependence of net uptake rates (F_1) on the intracellular palmitate concentration (C_i). Data from 39 liver perfusion experiments, with albumin in the range between 1.5 and 500 μM and portal extracellular palmitate in the range between 10 and 600 μM. C_i and F_1 were calculated from the rate constants as described in Materials and Methods. The solid line is the fitted regression line, with $y = 0.031x - 0.0184$ ($n = 39$; $r = 0.90$).

Dependence of influx on the equilibrium free palmitate concentration

In Fig. 6 the influx rates shown in Fig. 4 (fixed albumin and variable palmitate) and Fig. 5 (variable albumin and palmitate) were represented against the equilibrium free palmitate concentration, calculated as described in Materials and Methods. Fig. 6 allows a direct comparison of the rates of influx obtained in both experimental protocols. It is clear that the maximal influx rates measured in the constant ratio experiments (○) are well below the majority of the rates measured in the constant albumin experiments (●——●). Moreover, the data points of the latter are a saturable function of the equilibrium free palmitate concentration. The relation, however, is not Michaelian, i.e., the curve cannot be described by the simple Michaelis-Menten equation, as revealed by the Hofstee-plot in Fig. 6B. The constant ratio data (○), on the other hand, deviate from the saturation curve, except for those points obtained at albumin concentrations close or equal to 150 μM.

Dependence of net uptake on intracellular palmitate

The intracellular concentration (C_i) calculated according to Eqn. 2 is an average over all cells. It represents the sum of free + protein-bound palmitate and also constitutes an average over all intracellular compartments (cytosol, mitochondria, etc). In Fig. 7, rates of palmitate uptake (F_3) for 39 perfusion experiments were plotted against the intracellular palmitate concentration (C_i). The highest intracellular concentration found was equal to 46 μM, or 28.3 nmol per gram liver. The data show considerable dispersion. The straight line is the fitted regression line, with a correlation coefficient of 0.90. It seems that in the range up to 46 μM, esterification of palmitate to palmitoyl-CoA is roughly proportional to the total intracellular concentration.

Discussion

The main results obtained in this work can be summarized as follows: (1) Influx and net uptake rates of palmitate do not vary proportionally to each other when the albumin or palmitate concentrations are varied. (2) Efflux of palmitate is significant for all albumin concentrations in the range between 1.5 and 500 μM. (3) At 150 μM albumin, net uptake rates are proportional to the total (bound plus free) extracellular palmitate concentration in the range up to 500 μM; the dependence of influx on the palmitate concentration is rather concave up. (4) When albumin and palmitate are both varied at an equimolar ratio, pseudo-saturation appears in both net uptake and influx rates; the influx rates, however, tend to decrease again at higher concentrations. (5) As expected, the intracellular palmitate concentration depends on albumin. At very low concentrations of the protein (1.5 μM) the intracellular concentration is practically equal to the extracellular one in spite of the intracellular removal process; at physiological albumin concentrations, however, the intracellular palmitate concentration is less than 2% of the extracellular one. (6) The rates of metabolic transformation are approximately proportional to the total, free plus bound, intracellular palmitate concentration.

The observation that palmitate efflux is significant confirms the early study of Goresky et al. [10] in the liver of anesthetized dogs and with albumin concentrations in the physiological range. Our study reveals, in addition, that this occurs even at very low albumin concentrations (1.5 μM). Another difference between our study and that of Goresky et al. [10] is that experiments in the isolated liver allow calculation of influx, efflux and net uptake rates. This is difficult to perform in the anesthetized animal, because a number of fatty acids is present and the rate constants measured for the labelled species reflect the interference of all other analogues present in the circulation.

The lack of proportionality between influx and net uptake found in this work, especially when the albumin concentration was varied, speaks against the use of net uptake rates in place of influx rates when studying transport phenomena [1–4,8,9]. Actually, the kinetics of influx and net uptake may be completely different (Figs. 4 and 5). In the past, however, transport equations have been fitted to net uptake curves [1], theoretical influx curves have been compared to net uptake data [4,8] and, more recently, change in net uptake rates, measured at different membrane potentials, have been attributed to changes solely in influx rates [9]. However, especially in the latter case, it seems reasonable to expect changes in both k_1 and k_2.

The intracellular pools (C_i) used in this study are calculated parameters and it seems appropriate at this point to compare these calculated values with experimental data in the literature. Cooper et al. [34] have recently measured intracellular pools under various conditions. At an albumin concentration of 200 μM and for portal palmitate concentrations of 400 and 800 μM they found intracellular palmitate pools of 15 and 31.8 nmol per gram liver, respectively. We have not performed experiments under exactly the same conditions, but data from the series of experiments with 150 μM albumin in the perfusate can be used for comparison. For portal palmitate concentrations of 300, 360, 440, 550 and 600 μM, the calculations yielded intracellular pools of 13.3, 15.9, 18.2, 24.3, and 28.3 nmol/g, respectively. Our calculated values are, thus, within the same range as those determined experimentally [34], a further favourable indication of the reliability of the rate constants determined employing the model of Goresky [10]. The other favourable indication, as already mentioned in Results, is the agreement between the net uptake rates calculated from the rate constants and from Eqn. 3, the latter being independent of Goresky's model.

The proportionality between net uptake (F_3) and the intracellular pool of palmitate (C_i) is a phenomenon which must be interpreted considering binding of palmitate to intracellular sites. The intracellular concentration, C_i, calculated according to Eqn. 2, represents an average over all cells and over all intracellular compartments and includes both free and bound palmitate (see Fig. 1). The free palmitate concentration is certainly much lower than the total concentration. A saturable function should only be expected if F_3 were plotted against the intracellular free palmitate concentration, because the free form is probably the substrate for the enzymatic system. The proportionality between F_3 and C_i is possibly the reason for the linear relation between F_3 and C_e in the constant albumin experiments (Fig. 4). In fact, a con-

stant relation between F_3 and C_i and between C_e and C_{if}, also implies a constant proportion between F_3 and C_e.

An important question which arises at this point concerns the interpretation of the kinetics of influx. The existence of a carrier system for long-chain fatty acids seems to be well established by experimental evidence, not only in the liver cells [6,7,30], but also in other types of mammalian cells [28,31,32]. The experimental evidence includes the isolation of a protein that binds long-chain fatty acids, including oleate and palmitate [7], sensitivity of transport to inhibitors [28], sensitivity to specific antibodies [7,32] and Michaelian saturation kinetics for zero-trans influx rates with respect to the free oleate concentration [7,32]. In principle, thus, the saturation function of Fig. 6 is consistent with previous experimental evidence. However, contrasting with the evidence obtained by Stremmel and co-workers [6,32] with oleate in isolated cells, the data points in Fig. 6 cannot be described by the simple Michaelis-Menten equation (constant albumin experiments) and are also not independent of the albumin concentration (constant ratio experiments). In other words, there is no inconditional correlation between the influx rates and the calculated equilibrium free palmitate concentrations. The phenomena underlying these observations in the perfused liver may be very complex. Two aspects will be examined here in some detail: (a) the equilibrium free palmitate concentration may not always be a good estimate for the true mean free palmitate concentration along the sinusoids [4,31,33]; (b) since a carrier is probably involved, trans-effects, i.e., acceleration or inhibition of the unidirectional fluxes across the membrane, caused by the presence of the solute in the opposite side [11,12], can occur. In both cases, a hypothetical Michaelian saturation curve would be distorted.

What the free palmitate concentration (C_{cf}) concerns, the equilibrium concentration is the only one which can be calculated. Equilibrium is a reasonable assumption when the rate of dissociation is fast compared to influx. Stremmel and co-workers [6,32] have measured zero-trans influx rates in cell suspensions with dissociation rates exceeding the rates of influx by two orders of magnitude. Additionally, during the measurement of the initial rates, only a relatively small fraction of the fatty acid had been transported into the cellular space [6,32]. In the perfused liver, where the extracellular space is only half that of the cellular one, extraction may be as high as 76% and dissociation of the albumin-fatty acid complex may become rate-limiting for influx [4,31]. If this occurs, the calculated equilibrium-free palmitate concentrations are overestimated and the data points of F_1 versus C_{cf} will describe a curve shifted to the right relative to the true concentration dependence. Limitation by dissociation is likely in the low concentration range, i.e., in the initial upslope, because of the lower concentrations of the albumin-fatty acid complex. This is true for both experimental protocols employed in this work. However, the initial upslope of the constant ratio experiments should be much more affected than that of the constant albumin experiments because of the higher extraction, which may also lead to partial limitation by flow. Limitation by dissociation, however, should decrease progressively as the concentration of complexed palmitate is raised from less than 10 μM to 500 μM or so. For this reason, it seems unlikely that the quite different final tendencies of the data points in both experimental protocols are due to limitation of influx by dissociation, because in both cases the rates of dissociation tend to increase as the concentration of palmitate increases.

Trans-effects have been generally found to occur in carrier mediated transport [11,12]. When influx is measured under zero-*trans* conditions (i.e., when $C_i = 0$), as it has been done for oleate transport by Stremmel and co-workers [6,32], trans-effects are absent and Michaelian kinetics can be expected. Michaelian kinetics can also be expected when the intracellular concentration remains constant [12] or when equilibrium exchange is being measured [16]. Under steady-state conditions, however, with the intracellular concentration varying simultaneously with the extracellular one, as in our experiments, the kinetics of influx becomes a function of both the extra- and intracellular concentrations. Unfortunately, it is extremely difficult, if not impossible, two evaluate the intracellular free palmitate concentrations (i.e., C_{if}). Only C_i can be calculated. The latter parameter varies differently in both experimental protocols as C_e is changed (see Figs. 4 and 5) and it is highly probable that C_{if} is also a complex function of the experimental conditions. If trans-effects are present, consequently, their influence on the influx kinetics should not be the same in both experimental protocols, especially in the high concentration range.

For all these reasons, thus, one cannot really expect inconditional correlation between influx rates and the equilibrium free palmitate concentrations in the perfused liver, inasmuch as other factors, such as limitation by diffusion through an unstirred layer at the cell surface [8] may additionally contribute to the overall kinetics.

Acknowledgements

This work was supported by grants from the Third World Academy of Sciences (TWAS), the Conselho Estadual de Ciência e Tecnologia (CONCITEC) and the Conselho Nacional de Desenvolvimento Científico e Tecnológico (CNPq). Andreas J. Schwab was, sequentially, a Deutsche Forschungsgemeinschaft Senior

Research Fellow and an Assistant Professor at the McGill University with support of the National Institutes of Health.

References

1 Weisiger, R., Gollan, J. and Ockner, R. (1981) Science 211, 1048–1051.
2 Weisiger, R.A., Gollan, J.G. and Ockner, R.K. (1982) in Progress in liver diseases (Popper, E. and Schaffner, F., eds.), pp. 71–85, Grune and Stratton, New York.
3 Forker, E.L. and Luxon, B.A. (1983) J. Clin. Invest. 72, 1764–1771.
4 Weisiger, R.A. (1985) Proc. Natl. Acad. Sci. USA 82, 1563–1567.
5 Stremmel, W., Potter, B.J. and Berk, P.D. (1983) Biochim. Biophys. Acta 756, 20–27.
6 Stremmel W., Strohmeyer, G. and Berk, P.D. (1986) Proc. Natl. Acad. Sci. USA 83, 3584–3588.
7 Stremmel, W., Strohmeyer, G., Borchard, F., Kochwa, S. and Berk, P.D. (1985) Proc. Natl. Acad. Sci. USA 82, 4–8.
8 Bass, L. and Pond, S.M. (1987) in Pharmacokinetics: Mathematical and statistical approaches to metabolism and distribution of chemicals and drugs (Pecile, A. and Rescigno, A., eds.), pp. 241–265, Plenum Press, London.
9 Weisiger, R.A., Fitz, J.G. and Scharschmidt, B.F. (1989) J. Clin. Invest. 83, 411–420.
10 Goresky, C.A., Daly, D.S., Mishkin, S. and Arias, I.M. (1978) Am. J. Physiol. 234, E542–E553.
11 Silverman, M. and Goresky, C.A. (1965) Biophys. J. 5, 487–509.
12 Lieb, W. (1982) in Red cell membranes. A methodological approach (Ellory, J.C. and Young, J.D., Eds.), pp. 135–164, Academic Press, London.
13 Goresky, C.A. (1963) Am. J. Physiol. 204, 626–640.
14 Bracht, A., Schwab, A.J. and Scholz, R. (1980) Hoppe-Seyler's Z. Physiol. Chem. 361, 357–377.
15 Schwab, A., Bracht, A. and Scholz, R. (1979) Eur. J. Biochem. 102, 537–547.
16 Bracht, A., Kelmer-Bracht, A., Schwab, A.J. and Scholz, R. (1981) J. Biochem. 114, 471–479.
17 Goresky, C.A., Bach, G.G. and Nadeau, B.E. (1973) J. Clin. Invest. 52, 991–1008.
18 Ishii, E.L., Schwab, A.J. and Bracht, A. (1987) Biochem. Pharmac. 36, 1417–1435.
19 Ferraresi-Filho, O., Ferraresi, M.L., Constantin, J., Ishii-Iwamoto, E.L., Schwab, A.J. and Bracht, A. (1989) Braz. J. Med. Biol. Res. 22, 139–143.
20 Scholz, R., Hansen, W. and Thurman, R.G. (1973) Eur. J. Biochem. 38, 64–72.
21 Dole, V.P. and Meinertz, H. (1960) J. Biol. Chem. 235, 2595–2599.
22 Tanaka, T., Kosaka, K., Hoshimaru, M. and Numa, S. (1979) Eur. J. Biochem. 98, 165–172.
23 Scholz, R., Schwabe, U. and Soboll, S. (1984) Eur. J. Biochem. 141, 223–230.
24 Goresky, C.A., Bach, G.G. and Rose, C.P. (1983) Am. J. Physiol. 244, G215–G232.
25 Meier, O. and Zierler, K.L. (1954) J. Appl. Physiol. 6, 731–744.
26 Björck, A. and Dahlquist, G. (1972) Numerische Methoden, R. Oldenburg, Munich.
27 Schwab, A.J. (1984) Math. Biosci. 71, 57–79.
28 Abumrad, N.A., Perkins, R.C., Park, J.H. and Park, C.R. (1981) J. Biol. Chem. 256, 9183–9191.
29 Spector, A.A., Fletcher, J.E. and Ashbrook, J.D. (1971) Biochemistry 10, 3229–3232.
30 Stremmel, W. and Theilmann, L. (1986) Biochim. Biophys. Acta 877, 191–197.
31 Sorrentino, D., Robinson, R.B., Kiang, C.L. and Berk, P.D. (1989) J. Clin. Invest. 84, 1325–1333.
32 Stremmel, W. (1987) J. Clin. Invest. 81, 844–852.
33 Weisiger, R.A. and Ma, W.L. (1987) J. Clin. Invest. 79, 1070–1077.
34 Cooper, R., Noy, N. and Zakim, D. (1987) Biochemistry 26, 5890–5896.